Locating low-ohmic Variations in Resistance using Electron Beam Induced Voltage Imaging

Andrew J. Smith[1], Andreas Rummel[1], Matthias Kemmler[1], Klaus Schock[1], Stephan Kleindiek[1]
[1]Kleindiek Nanotechnik, Aspenhaustr. 25, Reutlingen, Germany
Phone : (+49)71213453950, Email : info@kleindiek.com

***Abstract*—Locating 'soft' faults resulting from minor variations in resistance can be difficult using EBAC or RCI. Here, the authors explore the use of Electron Beam Induced Voltage for addressing these issues.**

Keywords—EBIV, Failure Analysis, Nanoprobing

I. Introduction

As the complexity of integrated devices increases, more and more often soft, difficult to find failures cause issues. In some cases, it is necessary to locate a minute change in resistance. Methods such as Electron Beam Absorbed Current (EBAC) [1] or Resistive Contrast Imaging (RCI) [2] are used to locate shorts and opens but fail when trying to pinpoint small variations in resistance. In this work, a method published some time ago by T Nokuo et al. [3], then referred to as Voltage Distribution Contrast (VDIC), is revisited. In this study, the preferred terminology is Electron Beam Induced Voltage (EBIV) imaging.

II. The EBIV Method

Experiments were performed using a modified Prober Shuttle nanoprobing platform with capability for low-noise signal management. The platform was installed on a Zeiss GeminiSEM 300 Scanning Electron Microscope (SEM). The signal leads from the probe tips were connected to a custom amplifying system for generating EBIV data. The EBIV amplifier provides gain levels between 10^3 and 10^6. It has a selectable bandwidth ranging from 100 Hz to 1 MHz. It's voltage measurement limit (including the sample and cabling) is < 50 nV@100 Hz.

In order to obtain EBIV images, a probe tip is touched down on the sample surface. As shown schematically in Fig. 1, the sample is grounded and the path to the probe tip is represented by a number of resistors. The electrons delivered by the scanning electron beam flow to ground and induce a potential drop. In the example shown here, a potential drop of 5 µV is measured at each resistor when assuming a 100 nA beam current.

Fig. 1: EBIV signal generation principle. The electrons delivered by the scanning electron beam (red) flow to ground (bottom left) and induce a potential drop.

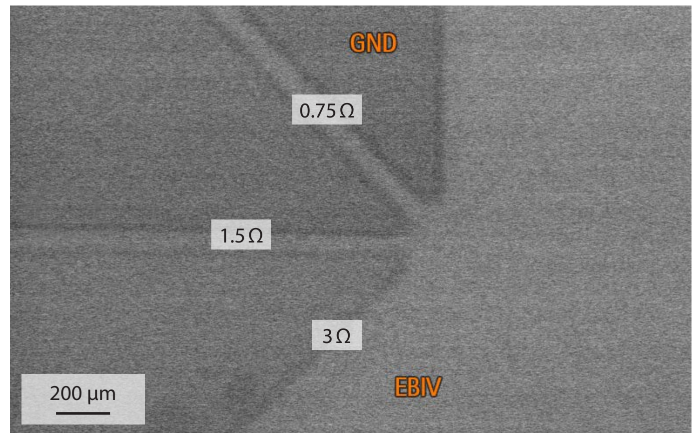

Fig. 2: SE image of a segmented sample separated by different resistors used to characterize the EBIV measurements recorded at 30 kV with a 120 µm aperture. The insets show the difference in resistance between the visible pads. The orange labels show where the probe tips were in touch with the sample.

III. EBIV Resolution

A sample with areas of identical SE emission that are connected by varying resistor values was used to estimate the expected resolution (Fig. 2). Two probe tips were touched down on the sample: One at the "12 o'clock" position connected to ground (GND), the other at the "6 o'clock" position connected to the EBIV amplifier.

The result shown in Fig. 2 shows that changes in resistance as low as 1.5 Ohm can be distinguished by the change in gray value in the EBIV image. The current generated by the electron beam (30 kV, 120 µm aperture) was measured to be 67 nA.

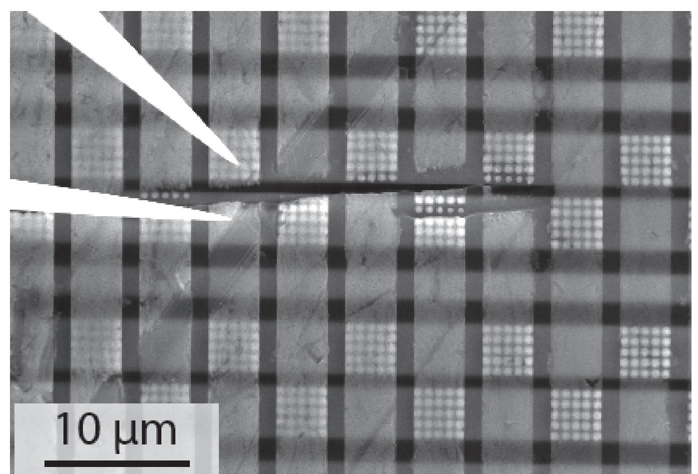

Fig. 3: Metal grid structure imaged in the SEM using a 30 kV beam to reveal the underlying grid structure. The two probe tips used to contact the sample are visible on the image's left-hand side.

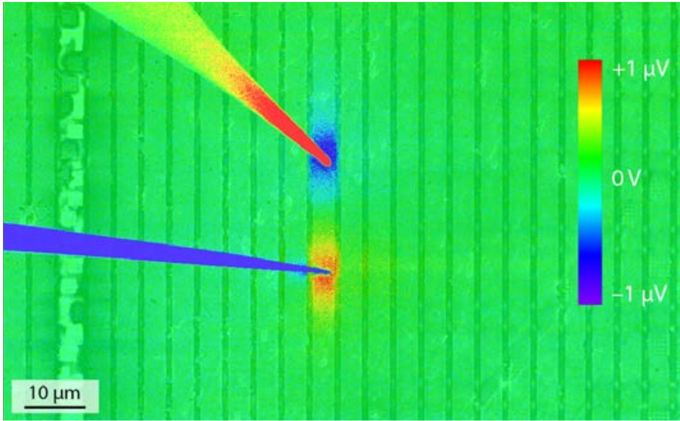

Fig. 4: EBIV image superimposed on the corresponding secondary electron (SE) image.

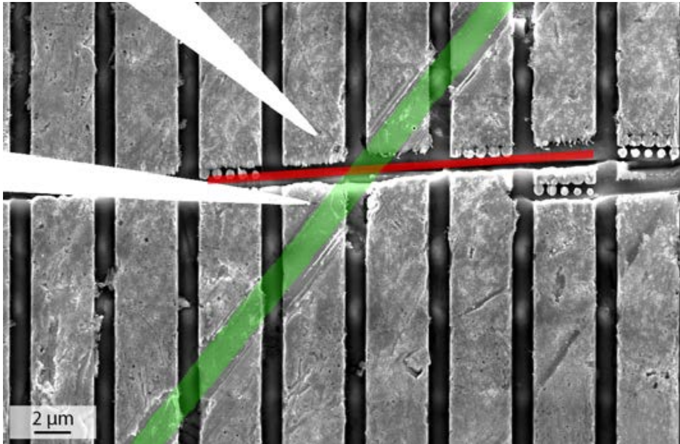

Fig. 5: SE image showing the location of a FIB cut (marked in red) and a scratch (marked in green).

IV. The Sample under Test

The sample used for the measurements was an Exynos 8895 device where an upper, multi-layer metal grid structure was addressed using two probe tips. The structure consists of multiple layers of parallel metal lines – each layer's lines perpendicular to the layer above and periodically connected with a matrix of 5 x 5 vias (Fig. 3). The sample was cut using a Focused Ion Beam (FIB) microscope in order to introduce a well-defined fault.

V. Detecting Low-ohmic Failures using EBIV

Initial measurements on undamaged metal lines illustrate the EBIV principle (Fig. 4). The upper needle in Fig. 4 is connected to GND, the lower needle is connected to the EBIV amplifier.

Measurements were also performed on the sample described in Fig. 3 at a site where mechanical defects (cuts, scratches) were present (Fig. 5). Two probes were touched down on the sample surface as shown in the schematic representation (Fig. 6). One probe tip had a low-ohmic connection to ground (GND), the other was connected to the EBIV amplifier's high-ohmic input.

The available current paths and corresponding voltage drops are illustrated schematically in Fig. 6 where the sample has a well-defined open. The EBIV amplifier‘s input is high-ohmic so that the current flow in the left probe tip is negligible. When the electron beam hits the sample, all current will flow to ground along the vias to the GND needle. The resulting voltage drop stems from this electron flow to the EBIV system‘s ground (GND) connection. The EBIV result in Fig. 7 (superimposed on the corresponding SE image) shows the voltage drops that occur along the contacted metal line. The image shows that there is no

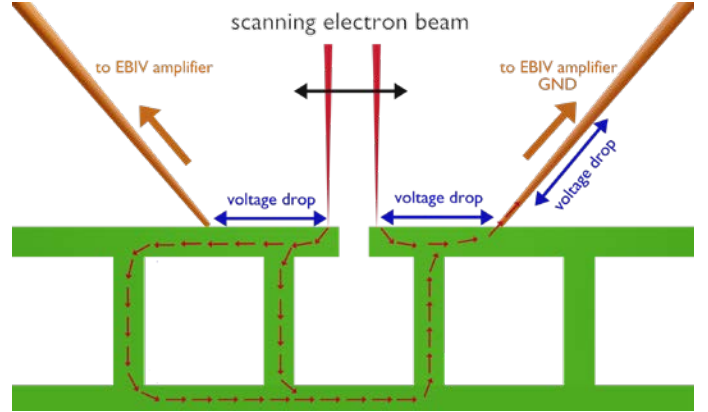

Fig. 6: EBIV schematic for the sample under test. Possible current paths for the electrons delivered by the electron beam are shown in red. The various voltage drops due to the sample's and tips' resistances are shown in blue.

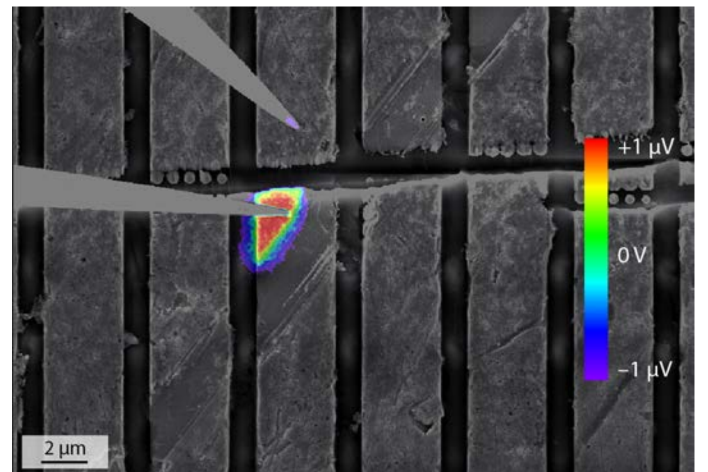

Fig. 7: EBIV data recorded at an acceleration voltage of 10 kV superimposed on the SE image (Fig. 5). The voltage contrast ends abruptly with the FIB cut but dissipates over approx. 1 µm at the scratch.

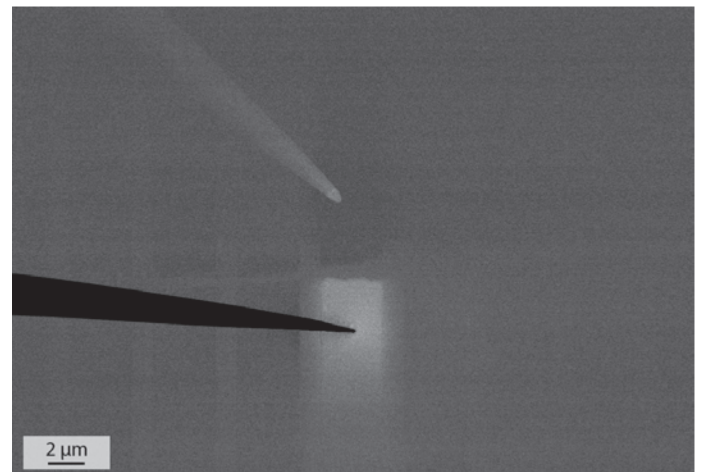

Fig. 8: Same experiment as shown in Fig. 7 on a site without scratches. The cut is still visible.

Fig. 9: Four-point resistance measurement yielding a resistance of 1.07 Ohm across the FIB cut.

voltage measured across the FIB cut – as expected. At the same time a voltage drop is seen below the FIB cut, the shape of which adheres to the scratch highlighted in green in Fig. 5.

On the other hand, a similar measurement performed on a metal line that was not scratched but cut using a FIB, shows an even voltage drop (Fig. 8).

VI. Discussion

In order to estimate the achieved resolution a resistance measurement was done (Fig. 9). Initially a two-point measurement was performed yielding an overall resistance of 39 Ohm. This includes the signal leads (approx. 3 Ohm each) as well as the contact resistances (approx. 16 Ohm each). An additional four-point measurement resulted in a resistance of 1.07 Ohm across the cut.

The EBIV measurement on the intact metal line (Fig. 4) shows a contrast change on both the metal line and at the contact point between tip and metal line. Two unexpected observations give rise to a closer examination:

1. The brightness (voltage) does not monotonically change from red to blue from the base of the EBIV needle to the base of the GND needle. It exhibits multiple inversions.
2. The brightness change across the 1.07 Ohm gap in Fig. 7 is much larger than expected as the resolution was determined to be approx. 1 Ohm (Fig. 2).

In order to examine these observations two probe tips were brought in contact to each other without touching the sample or anything else and EBIV images of the contact were recorded (Fig. 10).

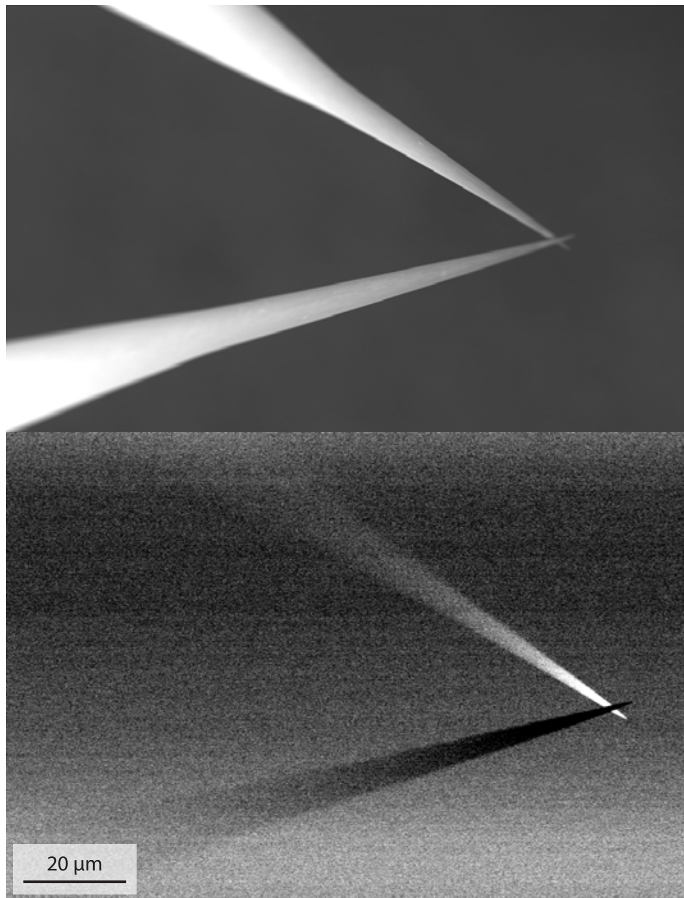

Fig. 10: SE image (top) and EBIV image (bottom) of two probe tips in contact with each other. Both images were recorded at an acceleration voltage of 10 kV. Measured resistance 6.90 Ohm

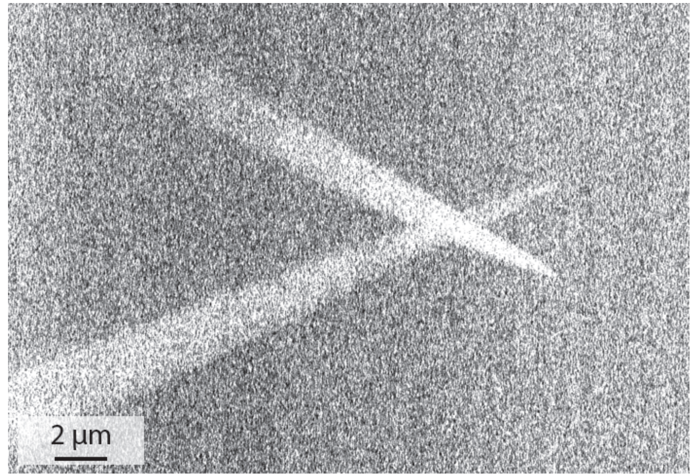

Fig. 11: EBIV image of two probe tips after tip cleaning in order to minimize the contact resistance. Image recorded at an acceleration voltage of 10 kV. The resulting resistance was 6.38 Ohm

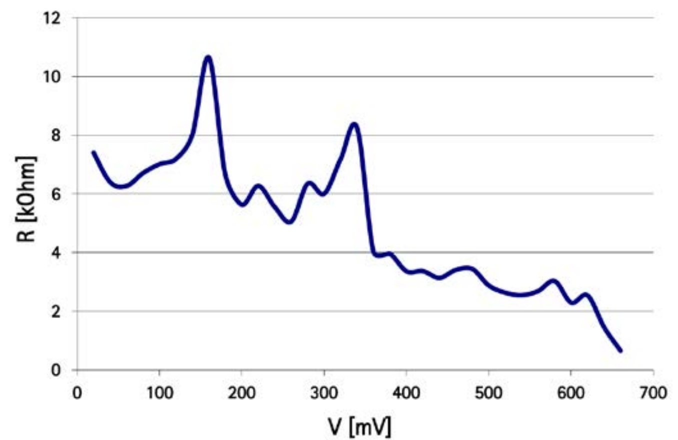

Fig. 12: I-V curve of a contact between two probe tips showing a voltage dependent resistance

A tip cleaning module (Kleindiek Nanotechnik) was used to generate lower contact resistances in a stepwise fashion. This was achieved by driving a controlled current through the tips in three steps resulting in series of ever decreasing resistances. The values measured by a digital multimeter (DMM) were 6.46 Ohm, 6.42 Ohm, and 6.38 Ohm (including the leads which contribute approx. two times 3 Ohm). The final EBIV image recorded at a resistance of 6.38 Ohm is shown in Fig. 11.

The smaller the contact resistance the smaller the brightness change at the contact. At 6.38 Ohm the contrast change at the tip nearly vanishes leading to the assumption that the contact resistance plays an important role for the EBIV image generation. However, this can neither explain the brightness change quantitatively nor the observed contrast reversal.

Measuring I-V curves of a contact between two tips at low voltages shows that the resistance at these low voltages can be more than ten times higher than the resistance at large voltages. This can be measured reversibly as long as the threshold for voltage breakthrough is not exceeded.

Fig. 12 shows that the resistance between two probe tips can vary by more than one order of magnitude depending on the applied voltage. We assume that the resistance of the EBIV measurement behaves in a similar way. The resistance is large as long as small voltages and currents are involved but is small if a voltage of around one volt is applied e.g. by a DMM.

VII. Secondary Electron Enhanced EBIV Signals

Referring to Fig. 10, the reversal in contrast to what was expected can be explained as follows: Initially, the effect of the primary electron beam is discussed while ignoring secondary electrons.

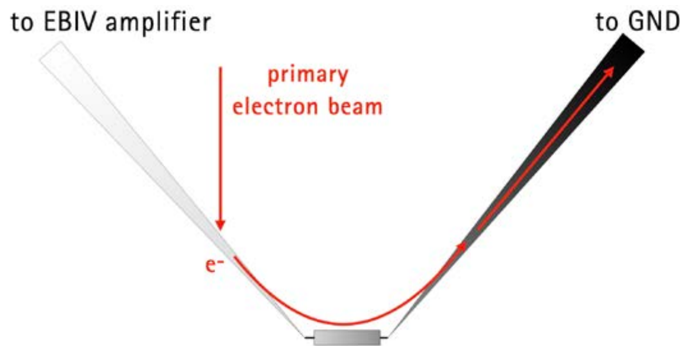

Fig. 13: Primary beam impinging on the EBIV probe needle - ignoring secondary electrons..

Primary electrons hitting the left probe needle (see Fig. 13) flow to the GND needle on the right hand side. The left needle is connected to the EBIV amplifier's high-ohmic input and measures the voltage generated by the electrons that flow through the contact resistance. Electrons flowing through the contact resistance to GND produce a negative voltage at the amplifier. Negative voltages are displayed as lighter gray values in the EBIV image.

The left needle in Fig. 14 is connected to the high-ohmic input of the EBIV amplifier and measures the voltage generated by the electrons that flow through the contact resistance. In addition to the previous images the backscattered and secondary electron emission is considered. Depending on the beam voltage and material (in this case: tungsten) more electrons can leave the probe tip than are induced by the primary electron beam causing a net loss of electrons remaining at the point where the electron beam hits the probe tip. In order to equalize this loss, electrons flow across the contact resistance from the reservoir of electrons at GND (right probe needle) to this point. Electrons flowing through the contact resistance from the GND produce a positive voltage at the amplifier. Positive voltages are displayed as dark gray values in the EBIV image.

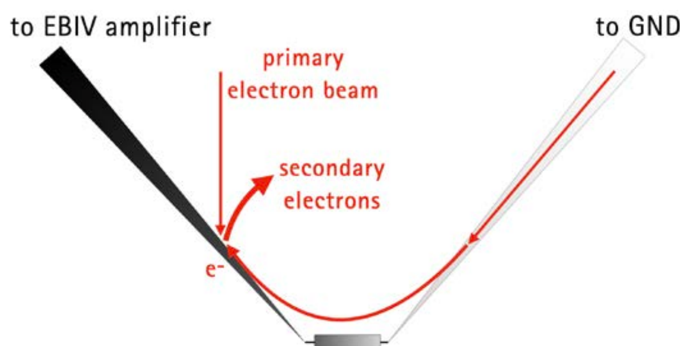

Fig. 14: Primary beam impinging on the EBIV probe needle - taking secondary electrons into account.

As the probe tip diameter gets smaller the secondary electron emission increases, thus resulting in a larger net loss of electrons at the point where the electron beam hits the probe tip (Fig. 15). In order to equalize this loss more electrons flow across the contact resistance from the reservoir of electrons at GND (right probe needle) to this point. More electrons flowing through the contact resistance from the GND produce a larger positive voltage change at the amplifier and cause the tip of the left probe needle to appear darker in the EBIV image than the thicker part of the needle.

In Fig. 16 the backscattered and secondary electron emissions are considered for the primary beam interacting with the GND probe tip. In order to equalize this loss, electrons flow from the GND reservoir of the right probe needle to the point where the primary electron beam penetrates the right probe tip. As these electrons from GND do not flow through the contact resistance, no voltage change can be measured at the EBIV amplifier's high-ohmic input and the needles appear uniformly gray (a very small voltage drop is caused by the resistance (< 1 Ohm) of the GND needle and a small change in gray value should be observed, however, this cannot be resolved by the EBIV amplifier).

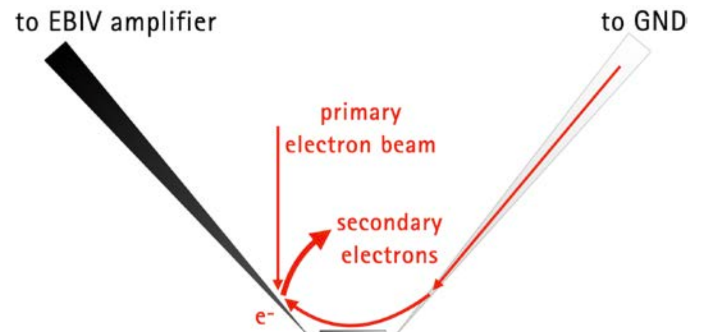

Fig. 15: Primary beam impinging on the EBIV probe needle close to the tip - taking secondary electrons into account.

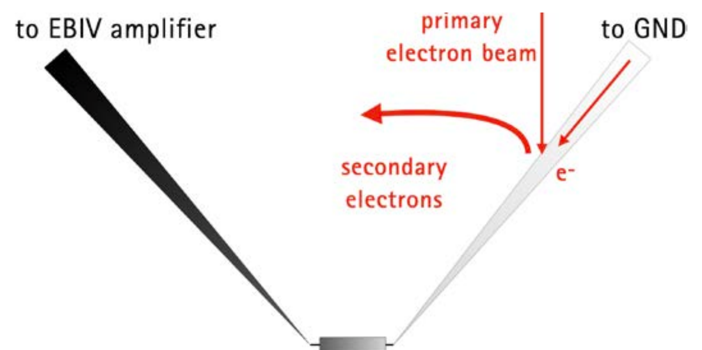

Fig. 16: Primary beam impinging on the GND probe needle - taking secondary electrons into account.

In addition to the previous image (Fig. 16) the primary electron beam hits the right probe needle close to the contact point and the backscattered and secondary electrons can reach the (left) EBIV needle (Fig. 17). As the EBIV needle is high-ohmic these

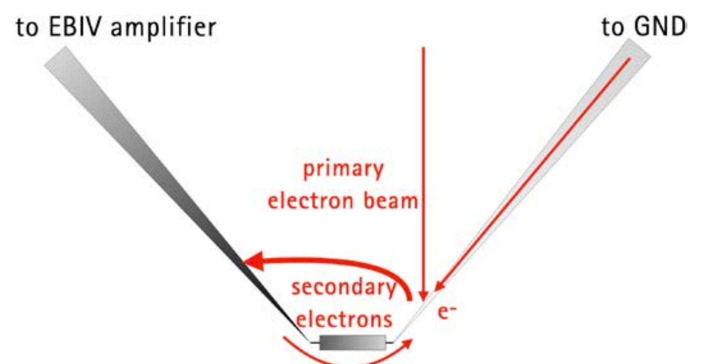

Fig. 17: Primary beam impinging on the GND probe needle close to the tip - taking secondary electrons into account.

electrons flow through the contact resistance to GND and produce a negative voltage at the amplifier resulting in the tip of the GND probe needle appearing bright (negative voltages are displayed as bright gray values in the EBIV image).

VIII. Conclusions

With the EBIV method a resistance resolution of about 1 Ohm is possible where a brightness change in the EBIV image corresponds linearly to a resistance change of the measured structure. The resolution depends on the beam current and on the voltage noise between the two contacts. For reference: The beam current employed for determining the resistance resolution was approx. 20 nA. EBIV imaging on the metal lines was performed at a beam current of 1 nA.

An enhanced contrast could be observed resulting from small oxide layers between two metal contacts which lead to an increased voltage drop across the probe needles.

We have shown that the enhanced contrast arises from a nonlinear resistive contact between probe tip and sample and the emission of secondary and backscattered electrons causing an additional current through the contact.

In addition, secondary electrons emitted from the probe tips or sample can increase the contrast not only between the probe tips and the sample but also at the location of the sample in case the probe tips are positioned close to the failure.

This could be demonstrated by observing a 1.07 Ohm failure and an even lower-ohmic transition to a scratched part of a metal line. Future steps will include making further improvements to the EBIV amplifier (increased sensitivity, lower noise, ...) and seeking out more applications that could benefit from the EBIV technique.

References

[1] Akira Shimase et al., “Failure Analysis Navigation System - Connecting Hardware Analysis to Software Diagnosis” in Proceedings of the 32nd International Symposium for Testing and Failure Analysis, Nov 2006

[2] C. A. Smith et al., “Resistive contrast imaging: A new SEM mode for failure analysis,” in IEEE Transactions on Electron Devices, vol. 33, no. 2, pp. 282-285, Feb. 1986, doi: 10.1109/T-ED.1986.22479.

[3] T. Nokuo, “Fault site localization technique by imaging with nanoprobes” Proceedings 19th European Symposium on Reliability of Electron Devices, Failure Physics and Analysis, October 2008.